Tetrahedron Letters 55 (2014) 3218–3222

Contents lists available at ScienceDirect

Tetrahedron Letters

journal homepage: www.elsevier.com/locate/tetlet

A new colorimetric and fluorescent bifunctional probe for Cu^{2+} and F^{-} ions based on perylene bisimide derivatives

Yefeng Wang, Liang Zhang, Guanjun Zhang, Yue Wu, Shengying Wu, Jianjun Yu, Limin Wang *

Key Laboratory for Advanced Material, and Institute of Fine Chemicals, East China University of Science and Technology, 130 Meilong Road, Shanghai 200237, PR China

ARTICLE INFO

Article history:
Received 22 November 2013
Revised 21 March 2014
Accepted 31 March 2014
Available online 5 April 2014

Keywords:
Perylene bisimide derivatives
Colorimetric
Fluorescent
Bifunctional probe

ABSTRACT

A perylene bisimide derivative (PBI) based colorimetric and fluorescent bifunctional probe **PAM-PBI** was designed and synthesized. It was highly selective and sensitive for distinguishing both Cu^{2+} and F^{-} from other ions through a conspicuous change of UV–vis and fluorescence spectra. The recognition of Cu^{2+} by **PAM-PBI** showed an obvious color change from rose red to purple in aqueous solution, while the sensing of F^{-} gave a marked color change from rose red to light green in THF.

Fluorescent chemosensors are widely used as powerful tools of recognizing and sensing cations and anions owing to their high sensitivity, selectivity, versatility, and relatively simplicity.[1] In particular, the design of sensors capable of recognizing and sensing both cations and anions, which are also called bifunctional probes, is one of the most challenging fields because of their significance in biological, chemical, and environmental processes.[2–6]

Copper, as the third most abundant element (after Fe^{2+} and Zn^{2+}) among essential heavy metal ions present in the human body, plays a critical role in many fundamental physiological processes.[7] Copper kills a variety of potentially harmful pathogens and hence has antimicrobial effect against MRSA, Escherichia coli, and other pathogens.[8–10] However, on excessive intake, Cu^{2+} causes injurious effects such as neurodegenerative diseases (e.g., Alzheimer's and Wilson's diseases) due to its participation in the production of reactive oxygen species.[11]

Additionally, fluoride has drawn wide attention thanks to its beneficial effects in preventing dental caries and in the treatment of osteoporosis.[12,13] Moreover, fluoride ions are associated with anesthetics, hypnotics, psychiatric drugs, nerve gases, in the analysis of drinking water and in the refinement of uranium used in nuclear weapon manufacture. Nevertheless, when administrated in high dose, it is dangerous and can lead to dental or skeletal fluorosis.[14,15]

Thus, the diversity of their functions, both beneficial and otherwise, makes the detection of copper and fluoride ions important. Consequently, considerable effort has been devoted to the design of fluorescent sensors for Cu^{2+} and F^{-}.[16–25]

Perylene dianhydride (PTCDA) and its derivatives (PBIs), as a representative of strongly fluorescent high performance pigments, have excellent chemical, thermal, photo, and weather stability.[26] In addition to their use as important industrial pigments, many PBIs also exhibit near-unity fluorescence quantum yields, high photochemical stability, and strong electron-accepting character. In this case, significant progress has been made to use PBIs-containing materials in organic field effect transistors (OFETs), fluorescent solar, collectors, electrophotographic devices, dye lasers, organic photovoltaic cells (OPVs), and optical power limiters.[27–29] Thanks to their excellent optical and electrical properties, they can be used as good platforms in the design of fluorescent sensors.[30–37] However, rare even none bifunctional chemosensors based on PBIs were reported.

Herein, we designed a new colorimetric and fluorescent bifunctional probe **PAM-PBI** for detection of both Cu^{2+} and F^{-} based on PBIs. It showed drastic fluorescence quench and obvious color change toward its binding of Cu^{2+} in buffered THF/MOPS (v/v = 4:1) solution and its interaction with F^{-} in THF with high selectivity and sensitivity.

PAM-PBI was obtained from **PTCDA** via imidization, nitration, reduction, and acetylation steps, as shown in Scheme 1 (Supplementary data).

Both UV–vis absorption and fluorescent emission studies revealed that **PAM-PBI** showed selectivity toward Cu^{2+} in THF/MOPS (v/v = 4:1, pH = 7.2) solution. As shown in Figure 1a, in the absence of Cu^{2+}, the maximum absorption wavelength of

---

* Corresponding author. Tel./fax: +86 21 64253881.
E-mail address: wanglimin@ecust.edu.cn (L. Wang).

http://dx.doi.org/10.1016/j.tetlet.2014.03.137

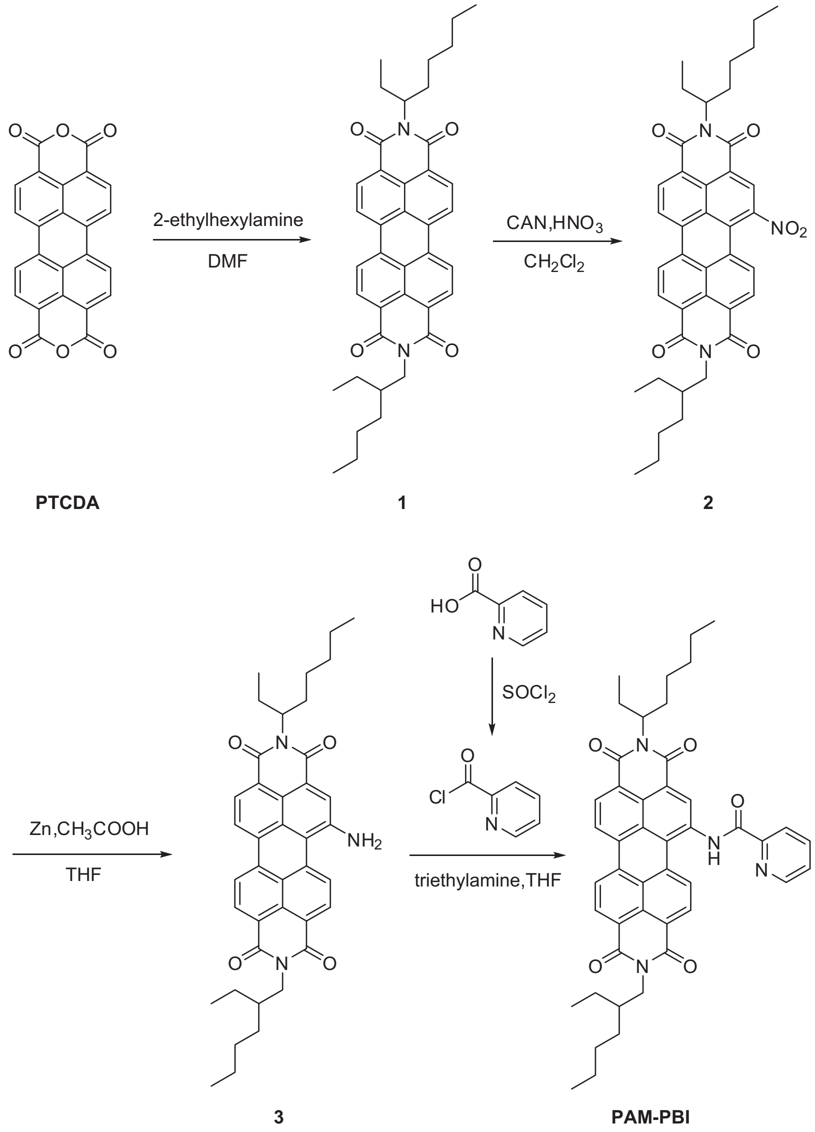

Scheme 1. The synthetic route of **PAM-PBI**.

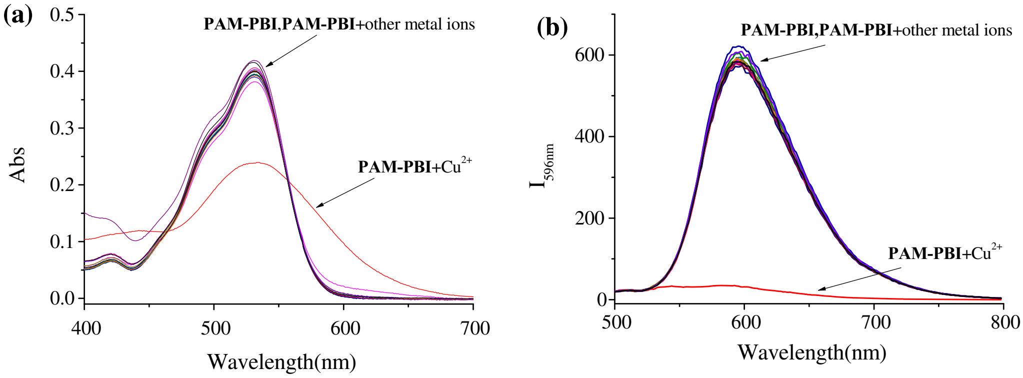

Figure 1. UV–vis (a) and fluorescence (b) spectra of **PAM-PBI** (10 μM) before and after adding 10 equiv of various cations (other metal ions: Ba^{2+}, Cd^{2+}, Ag^{+}, Pb^{2+}, Mg^{2+}, Mn^{2+}, Cr^{3+}, Zn^{2+}, Co^{2+}, Ni^{2+}, Fe^{2+}, Ca^{2+}, Hg^{2+}) in buffered THF/MOPS (v/v = 4:1) solution at pH 7.2.

PAM-PBI was at 531 nm (ε = 41,900). Subsequently, 10 equiv of different ions, such as Ba^{2+}, Cd^{2+}, Ag^{+}, Pb^{2+}, Mg^{2+}, Mn^{2+}, Cr^{3+}, Zn^{2+}, Co^{2+}, Ni^{2+}, Fe^{2+}, Ca^{2+}, and Hg^{2+} was added to measure the selectivity of **PAM-PBI** to Cu^{2+}. Upon addition of different metal ions, no obvious change of the absorption could be observed, while the addition of Cu^{2+} to **PAM-PBI** resulted in a slight bathochromic shift and synchronous decrease in the absorption band at 531 nm. Meanwhile, compared to other metal ions, only Cu^{2+} generated

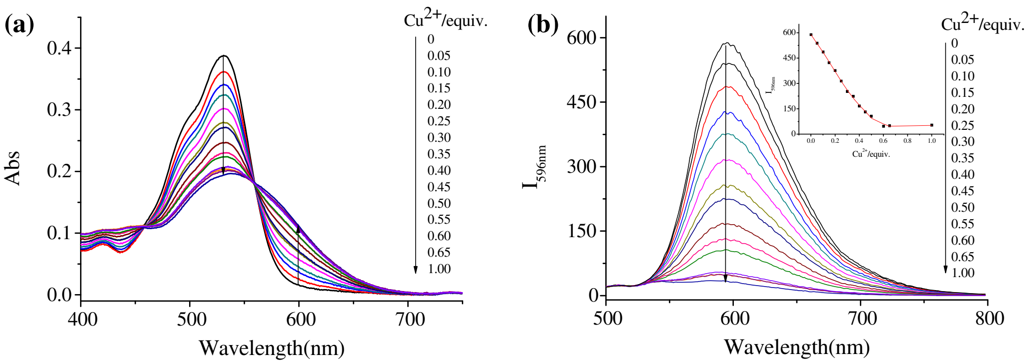

Figure 2. UV–vis (a) and fluorescence (b) spectra of **PAM-PBI** (10 μM) on addition of Cu^{2+} (0–1 equiv) in buffered THF/MOPS (v/v = 4:1) solution at pH 7.2. Inset: fluorescence intensity at 596 nm of **PAM-PBI** as a function of Cu^{2+} equivalent.

an approximately 27-fold fluorescence quench at 596 nm (Fig. 3b) (quantum yield, $\Phi_0 = 0.693$, $\Phi_1 = 0.026$). No significant fluorescence change was observed in the presence of other metal ions (Fig. 1b). These results demonstrated the high selectivity of **PAM-PBI** toward Cu^{2+}.

The absorption and fluorescence titration of Cu^{2+} was carried out using a solution of 10 μM **PAM-PBI** in THF/MOPS (v/v = 4:1). As illustrated in Figure 2, upon addition of increased amounts of Cu^{2+}, the absorbance of **PAM-PBI** at 531 nm decreased gradually and increased at a new band (>531 nm) without an obvious peak. The rose red solution of free **PAM-PBI** turned purple and exhibited two isosbestic points at 457 nm and 559 nm (Fig. 3a). Upon the excitation at 457 nm, the fluorescence intensity at 596 nm quenched linearly in the range of 0–0.5 equiv (Fig. S1). The linear equation was found to be $y = 524.08172 - 98.67246x$ ($R = 0.99186$), where y was the intensity at 596 nm measured at a given Cu^{2+} concentration and x represented the concentration (μM) of Cu^{2+} added. According to IUPAC, the detection limit was

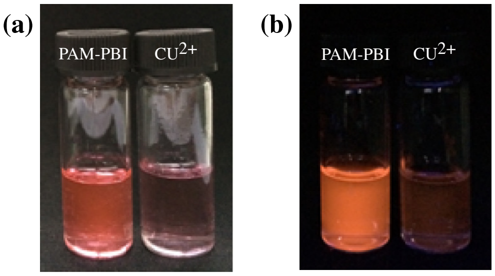

Figure 3. Color (a, left) and fluorescence (b, right) change of probe **PAM-PBI** upon addition of Cu^{2+} (1 equiv).

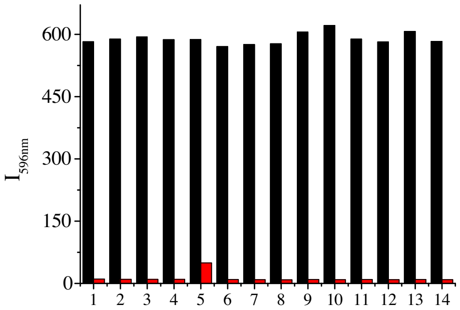

Figure 4. Fluorescence intensities of **PAM-PBI** (10 μM) in the presence of other related metal ions and Cu^{2+} mixtures in buffered THF/MOPS (v/v = 4:1) solution at pH 7.2. The black bars represent the emission intensities of **PAM-PBI** or **PAM-PBI** in the presence of different metal ions, the red bars represent the emission intensities of **PAM-PBI** in the presence of different metal ions (100 μM) and Cu^{2+} (10 μM). 1: no metal ion; 2: Pb^{2+}; 3: Mg^{2+}; 4: Mn^{2+}; 5: Cr^{3+}; 6: Zn^{2+}; 7: Co^{2+}; 8: Fe^{2+}; 9: Cd^{2+}; 10: Ba^{2+}; 11: Ni^{2+}; 12: Zn^{2+}; 13: Ca^{2+}; 14: Hg^{2+}.

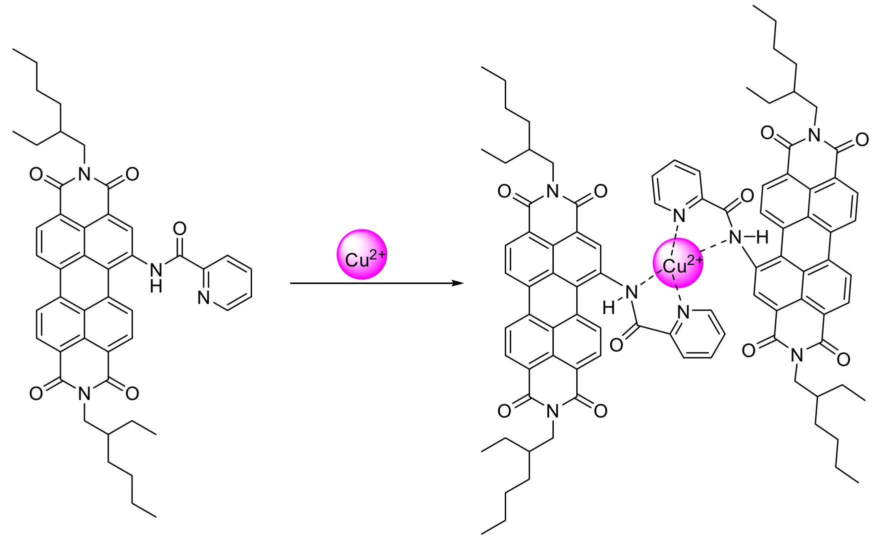

Scheme 2. Graphic of proposed mechanism of sensing Cu^{2+}.

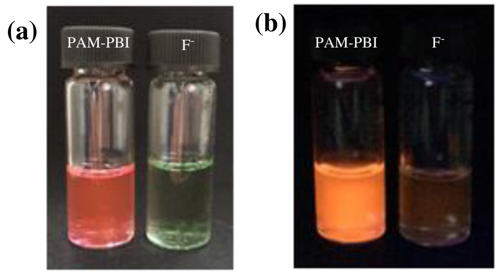

Figure 5. Color (a, left) and fluorescence (b, right) change of probe **PAM-PBI** upon addition of F^- (15 equiv).

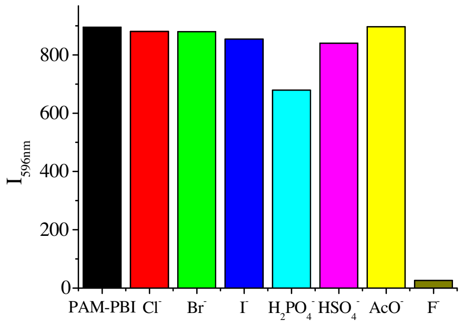

Figure 6. Selectivity of **PAM-PBI** (10 μM) upon addition of different anions (15 equiv) in THF.

determined from three times the standard deviation of the blank signal (3s) as 0.17 mM. Every measure mentioned above was finished within 1 min, which meant the sensor is real-time. These results proved that **PAM-PBI** could serve as a sensitive fluorescent probe for Cu^{2+}. According to Job's plot (Fig. S2), **PAM-PBI** and Cu^{2+} formed a 2:1 stoichiometry complex, as shown in Scheme 2. The binding mode of **PAM-PBI** and Cu^{2+} was confirmed by MALDI-TOF-MS (Supplementary data) in which a maximum peak is found at *m*/*z* 1531.6 [(2**PAM-PBI** + Cu^{2+} + H^-)$^+$].

The quenching phenomenon could be explained by two factors. Firstly, Cu^{2+} bound to N atoms of the amide and pyridine moiety from two equivalent of **PAM-PBI**, which resulted in the energy transfer from **PAM-PBI** to Cu^{2+}. The second factor may be attributed to the paramagnetic property of Cu^{2+}.[38]

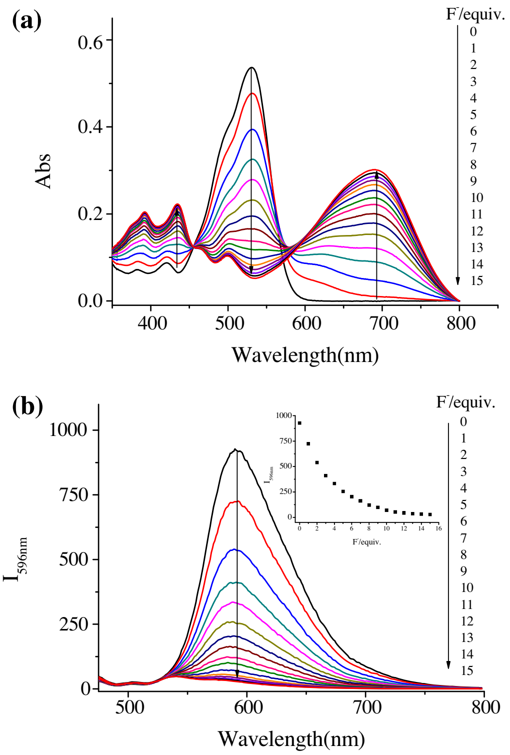

Figure 7. UV–vis (a) and fluorescence (b) spectra of **PAM-PBI** (10 μM) on addition of F^- (0–15 equiv) in THF. Inset: fluorescence intensity at 596 nm of **PAM-PBI** as a function of F^- equivalent.

To further examine the effective application of **PAM-PBI**, the competition experiment was carried out. As shown in Figure 4, in the presence of relevant analytes, the addition of Cu^{2+} still quenched the fluorescence of **PAM-PBI**, which indicated that the detection of Cu^{2+} was not interfered, thus **PAM-PBI** displayed a high selectivity for Cu^{2+} even under competition.

In addition to the cation binding properties, we also investigated the sensing properties of **PAM-PBI** for anions. 15 equiv of different anions (F^-, Cl^-, Br^-, I^-, S^{2-}, $H_2PO_4^-$, AcO^-) was added into 10 μM **PAM-PBI** in THF. UV–vis spectra (Fig. S3) showed that the absorption of **PAM-PBI** at 531 nm (ε' = 53,700) decreased prominently and a new absorption band at 692 nm appeared upon the addition of F^-, and the fluorescence intensity at 596 nm experienced a

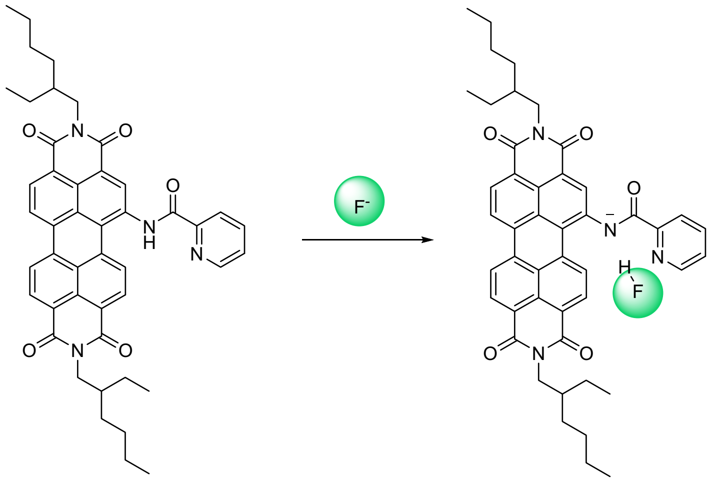

Scheme 3. Graphic of proposed mechanism of sensing F^-.

drastic quench (Fig. 5b) (quantum yield, $\Phi'_0 \sim 1$, $\Phi_2 = 0.093$). As a result, the solution color changed from rose red to light green (Fig. 5a). However, both absorbance and fluorescence intensity of **PAM-PBI** had no significant change toward the other anions (Figs. 6 and S4).

Upon the progressive addition of F^-, the peak at 531 nm decreased and a totally new band at 692 nm with a large bathochromic shift was developed gradually with two isosbestic points at 455 nm and 579 nm (Fig. 7). Meanwhile, the fluorescence intensity at 596 nm totally quenched with a nonlinear curve toward the concentration of F^-. Intermolecular proton transfer (IPT) process between the amide moiety and fluoride ion may be a possible explanation for the F^- anion-triggered spectroscopic changes (Scheme 3).[39] Actually, the quench process followed the modified Stern–Volmer relationship (Fig. S5), which meant the F^- accelerated the fluorescence quench of **PAM-PBI**. As shown in Figure S6, the *S*–*V* plot had been found to be nonlinear with an upward curvature and which obeyed the polynomial equation. The results suggested that both static and dynamic quenching processes were responsible for the observed positive deviation in the *S*–*V* plot.[40] From the titration experiment, the detection limit was calculated to be 22 μM.

In summary, we designed and synthesized a colorimetric fluorescent bifunctional probe based on PBIs, which showed different response toward Cu^{2+} in aqueous solution and F^- in THF with high selectivity and sensitivity. To the best of our knowledge, it may be the first bifunctional probe based on PBIs ever reported. Moreover, it has potential application as a dual output molecular switch due to its bifunction.

Acknowledgments

The work was supported by the National Nature Science Foundation of China (NSFC, 21272069, 20672035), the Fundamental Research Funds for the Central Universities and Key Laboratory of Organofluorine Chemistry, Shanghai Institute of Organic Chemistry, Chinese Academy of Sciences.

Supplementary data

Supplementary data (Supplementary material contains detailed synthesis process, ^1H NMR, HRMS spectra of **PAM-PBI** and Figs. S1–S6.) associated with this article can be found, in the online version, at http://dx.doi.org/10.1016/j.tetlet.2014.03.137.

References and notes

1. de Silva, A. P.; Gunaratne, H. Q. N.; Gunnlaugsson, T. A.; Huxley, J. M.; McCoy, C. P.; Rademacher, J. T.; Rice, T. E. *Chem. Rev.* **1997**, *97*, 1515.
2. Valeur, B.; Leray, I. *Coord. Chem. Rev.* **2005**, *205*, 3.
3. Gale, P. A. *Coord. Chem. Rev.* **2003**, *240*, 191.
4. Haas, K. L.; Franz, K. J. *Chem. Rev.* **2009**, *109*, 4921.
5. Okamoto, A.; Ichiba, T.; Saito, I. *J. Am. Chem. Soc.* **2004**, *126*, 8364.
6. Gadd, G. M. *Microbiology* **2010**, *156*, 609.
7. Linder, M. C.; Wooten, L.; Cerveza, P.; Cotton, S.; Shulze, R.; Lomeli, N. *Am. J. Clin. Nutr.* **1998**, *67*, 965S.
8. Noyce, J. O.; Michels, H.; Keevil, C. W. *J. Hosp. Infect.* **2006**, *63*, 289.
9. Noyce, J. O.; Michels, H.; Keevil, C. W. *Appl. Environ. Microbiol.* **2006**, *72*, 4239.
10. Mehtar, S.; Wiid, I.; Todorov, S. D. *J. Hosp. Infect.* **2008**, *68*, 45.
11. Muthaup, G.; Schlicksupp, A.; Hess, L.; Beher, D.; Ruppert, T.; Masters, C. L.; Beyreuther, K. *Science* **1996**, *271*, 1406.
12. Kirk, K. L. *Biochemistry of Halogens and Inorganic Halides*; Plenum: New York, 1991. P 58.
13. Kleerekoper, M. *Endocrinol. Metab. Clin. North Am.* **1998**, *27*, 441.
14. Matuso, S.; Kiyomiya, K.; Kurebe, M. *Arch. Toxicol.* **1998**, *72*, 798.
15. Barbier, O.; Arreola-Mendo, L. *Chem. Biol. Interact.* **2010**, *188*, 319.
16. Dalapati, S.; Jana, S.; Alam, M. A.; Guchhait, N. *Sens. Actuators B: Chem.* **2011**, *160*, 1106.
17. Zou, Q.; Li, X.; Zhang, J.; Zhou, J.; Sun, B.; Tian, H. *Chem. Commun.* **2012**, 2095.
18. Chen, Z.; Wang, L. *Spectrochim. Acta A* **2013**, *105*, 57.
19. Wade, C. R.; Broomsgrove, A. E. J.; Aldridge, S.; Gabbai, F. P. *Chem. Rev.* **2010**, *110*, 3958.
20. Ren, J.; Wu, Z.; Zhou, Y.; Li, Y.; Xu, Z. *Dyes Pigm.* **2011**, *91*, 442.
21. Jiang, Y.; Zhao, H.; Lin, Y.; Zhu, N.; Ma, Y.; Mao, L. *Angew. Chem., Int. Ed.* **2010**, *122*, 4910.
22. Zhang, J. F.; Lim, C. S.; Bhuniya, S.; Cho, B. R.; Kim, J. S. *Org. Lett.* **2011**, *13*, 1190.
23. Sokkalingam, P.; Lee, C. H. *J. Org. Chem.* **2011**, *76*, 3820.
24. Qu, Y.; Hua, J.; Tian, H. *Org. Lett.* **2010**, *12*, 3320.
25. Huang, C.; Barlow, S.; Marder, S. R. *J. Org. Chem.* **2011**, *76*, 2386.
26. Ahrens, M. J.; Fuller, M. J.; Wasielewski, M. R. *Chem. Mater.* **2003**, *15*, 2684.
27. Gvishi, R.; Reisfeld, R.; Burshtein, Z. *Chem. Phys. Lett.* **1993**, *213*, 338.
28. Anthony, J. E. *Chem. Mater.* **2011**, *23*, 583.
29. Feng, L.; Chen, Z. *Sensors Actuators B: Chem.* **2007**, *122*, 600.
30. Yan, L.; Yang, L.; Lan, J.; You, J. *Sci. China, Ser. B: Chem.* **2009**, *52*, 518.
31. Soh, N.; Ariyoshi, T.; Fukaminato, T.; Nakano, K.; Irie, M.; Imato, T. *Bioorg. Med. Chem. Lett.* **2006**, *16*, 2943.
32. Soh, N.; Ariyoshi, T.; Fukaminato, T.; Nakajima, H.; Nakano, K.; Imato, T. *Org. Biomol. Chem.* **2007**, *5*, 3762.
33. Ito, F.; Ariyoshi, T.; Soh, N.; Kakiuchi, T.; Inoue, T.; Imato, T. *Chem. Lett.* **2008**, *37*, 1202.
34. Ruan, Y.; Li, A.; Zhao, J.; Shen, J.; Jiang, Y. *Chem. Commun.* **2010**, 4938.
35. Miyake, Y.; Togashi, H.; Tashiro, M.; Yamaguchi, H.; Oda, S.; Kudo, M. *J. Am. Chem. Soc.* **2006**, *128*, 2172.
36. He, X.; Zhong, Z.; Guo, Y.; Lv, J.; Xu, J.; Zhu, M. *Langmuir* **2007**, *23*, 8815.
37. Zhang, L.; Wang, L. *Tetrahedron Lett.* **2013**, *54*, 4019.
38. Wang, H.; Xue, L.; Fang, Z.; Li, G.; Jiang, H. *New J. Chem.* **2010**, *34*, 1239.
39. Chen, Z.; Wang, L. *Dyes Pigm.* **2012**, *94*, 410.
40. Lakowicz, J. R. *Principles of Fluorescence Spectroscopy*; Plenum: New York, 1986.